Eur. J. Biochem. **268**, 389–395 (2001) © FEBS 2001

Solution structure of human immunodeficiency virus type 1 Vpr(13–33) peptide in micelles

Andrea Engler[1], Thomas Stangler[2] and Dieter Willbold[2]

[1]*Lehrstuhl für Biopolymere, Universität Bayreuth, Germany;* [2]*Institut für Molekulare Biotechnologie, Jena, Germany*

Human immunodeficiency virus type 1 protein R (HIV-1 Vpr) promotes nuclear entry of viral nucleic acids in nondividing cells, causes G_2 cell cycle arrest and is involved in cellular differentiation and cell death. Also, Vpr subcellular localization is as variable as its functions. It is known that, consistent with its role in nuclear transport, Vpr localizes to the nuclear envelope of human cells. Further, a reported ion channel activity of Vpr obviously is dependent on its localization in or at membranes. We focused our structural studies on the secondary structure of a peptide consisting of residues 13–33 of HIV-1 Vpr in micelles. Employing nuclear magnetic resonance and circular dichroism spectroscopy we found this part of Vpr, known to be essential for nuclear localization, to be almost completely α helical. Our results provide structural data suggesting residues 13–33 of Vpr to form an amphipathic, leucine-zipper-like α helix that serves as a basis for interactions with a variety of viral and cellular factors.

Keywords: HIV-1; Vpr; peptide solution structure; dodecylphosphocholine; micelles.

Human immunodeficiency virus type 1 (HIV-1) is a member of the lentivirus family. In addition to the *gag, pol* and *env* genes present in all retroviruses, HIV-1 encodes regulatory and accessory proteins, that are decisive for viral infectivity, replication and pathogenity. One of these proteins is virus protein R (Vpr). Vpr seems to be required at various steps of the HIV replication cycle and is therefore an interesting target for the development of antiviral agents. This 96-amino-acid protein is an important factor for the pathogenicy of HIV [1,2]. Vpr is an integral part of viral particles suggesting an important role in early stages of infection [3–6]. Furthermore, Vpr is involved in the transport of the preintegration complex into the host cell nucleus, which is an important feature for infection of nondividing cells [7,8]. Vpr causes changes in cell morphology [9] and arrests mammalian and yeast cells in G_2 phase of the cell cycle [10–13]. Further, Vpr has been proposed to have ion-chanel activity [14,15].

Different cellular proteins are reported to interact with Vpr: uracil DNA glycosylase [16], HHR23A, a protein implicated in DNA repair [17], a 41-kDa cytosolic protein that coprecipitates with the glucocorticoid receptor [18], importin-α, nuclear pore protein Nsp1p [19], and many others.

Recent structural studies of Vpr fragments by NMR were performed in trifluoroethanol (30%) containing solution and, not surprisingly, revealed a long amphipathic α helix-turn-α helix (amino acids 17–46) motif ended by a turn for Vpr (1–51) [20]. The Vpr (52–96) fragment, also in trifluorethanol containing solution, is characterized by an amphipathic α helix from residue 53 to residue 78 and a less defined C-terminal domain [21]. Another fragment of Vpr (50–82) was shown to contain a helix from residues 53–81 in 50% trifluorethanol. Trifluorethanol, however, is well known to induce α helical secondary structures in peptides [22].

We focused our structural studies on residues 13–33 of HIV-1 Vpr. This part of Vpr is known to be essential for ion chanel activity [15], cell cycle arrest [23], incorporation of Vpr into virus-like particles [24–26], and its nuclear localization [27]. Because a membranous or membrane-like environment may be important for most of these activities, we carried out structural studies of Vpr(13–33) peptide in dodecylphosphocholine (dodecyl-*P*Cho) containing micelles by CD and NMR spectroscopy.

MATERIALS AND METHODS

Peptide

The synthetic peptide CH_3CO-EPYNEWTLELLEELK-SEAVRH-NH_2 with the amino-acid sequence of HIV-1 Vpr(13–33) was purchased as a purified product (Interactiva, Ulm, Germany). N- and C-termini were modified by an acetyl and an amide group, respectively, to remove charges that are not present in the full length Vpr protein either. The peptide was more than 95% pure as judged from RP-HPLC analysis. Mass spectroscopy proved the product to have a mass of 2627.4 Da, close to the theoretical value (2626.9 Da).

Circular dichroism

CD spectra were recorded from 260 nm to 190 nm at 20 nm·min^{-1} on a Jasco J 810 CD spectropolarimeter. Samples contained 0.2 mg·mL^{-1} peptide in various

Correspondence to D. Willbold, Institut für Molekulare Biotechnologie, Strukturelle und Evolutive Biochemie, Beutenbergstr. 11, D-07745 Jena, Germany. Tel.: + 49 3641 65 6440, Fax: + 49 3641 65 6444, E-mail: willbold@imb-jena.de

Abbreviations: clean-TOCSY, TOCSY with suppression of NOESY-type crosspeaks; HIV, human immunodeficiency virus; Vpr, virus protein R.

(Received 13 October 2000, accepted 13 November 2000)

```
         10        20        30        40        50        60        70        80        90
         |         |         |         |         |         |         |         |         |
MEQAPEDQGPQREPHNEWTLELLEELKNEAVRHFPRIWLHGLGQHIYETYGDTWAGVEAIIRILQQLLFIHFRIGCRHSRIGVTQQRRARNGASRS

                hhhhhhhhhhhhhhhhhh  hhhhhhhhhhhhhh     hhhhhhhhhhhhhhhhhhhhh
```

Fig. 1. Secondary structure prediction. The amino-acid sequence of HIV-1 Vpr is shown according to the one-letter convention with residue numbers indicated above. Secondary structure prediction was carried out using the PHD NETWORK [41]. Three helices were predicted with the highest possible probability, indicated with 'h' below the sequence. The part of Vpr investigated in this work is indicated by a box.

solutions. The sample volume was 250 μL. The reference samples contained solute without peptide. Eight scans were accumulated from samples and references.

NMR spectroscopy

Sample concentrations used for NMR spectroscopy were 2.2 mM in 0.75 mL of H_2O/D_2O (9 : 1, v/v) and zero to 100 mM dodecyl-*P*Cho. Homonuclear 2D experiments were performed at 298 K on a Varian INOVA 600 spectrometer equipped with a triple-axis pulsed field gradient probe. A DQF-COSY [28] and a TOCSY [29] with 80 ms mixing time using the DIPSI mixing sequence [30] were recorded. NOESY spectra were recorded with 100 and 200 ms mixing times. All spectra were measured in the phase sensitive mode with quadrature detection in both dimensions using the States–TPPI method. Solvent suppression was performed by continuous coherent irradiation prior to the first excitation pulse and during the mixing time in the NOESY experiments. For the TOCSY experiment, the WATERGATE solvent suppression was used. All data sets were recorded with a 13.3 p.p.m. sweep width and contained 2048 or 1664 (F2) and 512 (F1) complex data points. Prior to Fourier transformation, the time domain signals were multiplied by a phase-shifted sine-bell-squared function. All NMR data were processed and analyzed with the program package NDEE (SpinUp Inc., Dortmund, Germany). Chemical shift values are reported in p.p.m. from 2,2-dimethyl-2-silapentanesulfonate.

Experimental restraints for structure calculation of Vpr(13–33) peptide

Distance information was extracted from the NOESY experiment with a mixing time of 100 ms. NOE cross peaks were categorized as 'strong', 'medium', and 'weak' and converted into upper limit distance constraints of 0.27, 0.41, and 0.51 nm, respectively. A total of 190 experimental restraints were used for the structure calculations. Only unambiguous distance restraints were included in the initial rounds of calculation. Very few additional distance restraints were included in several rounds of structure calculation after inspection of the initial structures [31].

Structure calculation and analysis

All structures were calculated using XPLOR 3.851 [32] and a modified *ab initio* simulated annealing protocol [33,34] that includes floating assignment of prochiral groups [35] and a reduced presentation for nonbonded interactions for part of the calculation [36]. Each round of the structure calculation started from templates with random backbone torsion angles. During all stages of the simulation, the temperature was maintained by coupling to a heat bath with a coupling frequency of 10 ps^{-1}. In the conformational search phase, 90 ps of molecular dynamics were simulated at 2000 K (3 fs timestep) computing nonbonded interactions only between C_α atoms and one carbon of each side-chain using van der Waals radii of 2.25 Å [36] in order to increase efficiency. The refinement comprised a two-phase cooling procedure treating explicitly the nonbonded interactions between all atoms. The first stage comprised cooling from 2000 K to 1000 K within 60 ps (2 fs timestep) and a gradual increase of the force constants for the nonbonded interactions and the angle energy constant for the diastereospecifically unassigned groups to their final values. In the next stage of the calculation, the system was cooled from 1000 K to 100 K within 40 ps (2 fs timestep), applying the high force constants obtained at the end of the previous cooling stage, followed by 200 steps of energy minimization.

Of the 160 structures resulting from the final round of structure calculation, those 22 structures that showed the lowest energy and no NOE distance violation larger than 0.02 nm were selected for further characterization. All calculations were carried out on Compaq DS20 server requiring an average of 3 min cpu time for each calculated structure. Geometry of the structures, structural parameters and elements of secondary structure were analyzed using the programs PROCHECK [37] and PROMOTIF [38]. For the graphical presentation of the structures, SYBYL 6.4 (Tripos Ass.), MOLSCRIPT, and RASTER3D were used. The

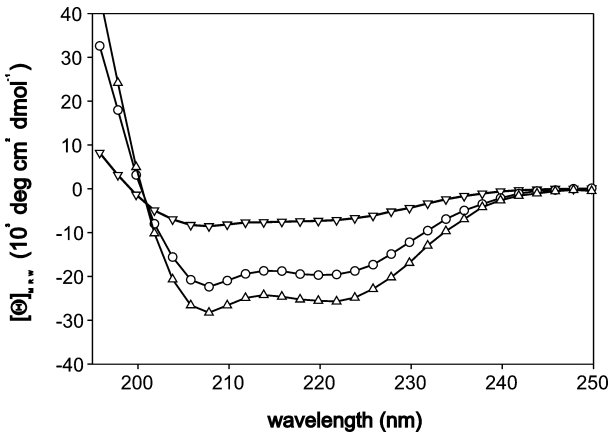

Fig. 2. Circular dichroism spectra of Vpr(13–33). CD spectra were recorded from 260 nm to 190 nm at 20 nm·min^{-1} on a Jasco J 810 CD spectropolarimeter. Samples contained 0.2 mg·mL^{-1} peptide. The sample volume was 250 μL. The reference samples contained solute without peptide. Eight scans were accumulated from samples and references. Shown are spectra of Vpr(13–33) in water (▽), trifluorethanol/water (1 : 1, v/v; △) and 100 mM dodecyl-*P*Cho (○).

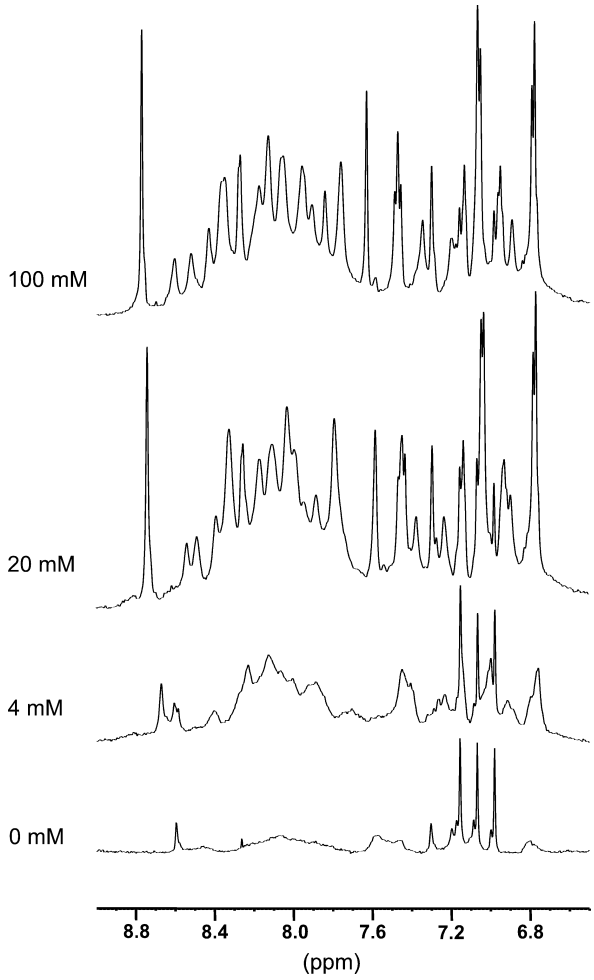

Fig. 3. ^{1}H-NMR titration of Vpr(13–33) with dodecyl-*P*Cho. 1D proton spectra of 2.2 mM Vpr(13–33) peptide at 298 K without dodecyl-*P*Cho (bottom) and with increasing concentrations of dodecyl-*P*Cho (shown on left hand side). Shown is the region of aromatic and amide protons.

coordinates have been deposited to the Protein Data Bank accession no. 1FI0 (available at http://www.rcsb.org/pdb/). Chemical shifts have also been deposited to the BioMagResBank with accession no. BMRB-4799 (available at http://www.bmrb.wisc.edu/pages/).

RESULTS

The N-terminal portion of Vpr (1–40) was reported to be responsible for ion chanel activity [15] and Vpr (17–33) for incorporation into virus-like particles [23–26], and for nuclear localization [27], and even for association with the nuclear envelope of human cells [19]. A membranous or membrane-like environment may be important for at least some of these activities.

In addition to previously reported secondary structure predictions, which only detected two helices [39,40], we used PHD NETWORKS, which has been reported to have an accuracy greater than 70% [41] for secondary structure prediction. This algorithm yielded three amphipathic helices: the first helix ranging from amino acid Asn16 to His33, the second helix from Arg36 to Thr49 and the third from Trp54 to Ile74 (Fig. 1).

As a result of the results from our secondary structure prediction analysis, we decided to focus our experimental studies on residues 13–33 of Vpr, which is very likely to comprise the part of Vpr essential its for membrane associated functions and investigated its behaviour under various solvent conditions.

CD spectra of Vpr(13–33) peptide in water does not show the presence of a significant amount of regular secondary structure (Fig. 2). In contrast, the peptide shows substantial content of α helical secondary structure in dodecylphosphocoline (dodecyl-*P*Cho) micelles and 1 : 1 (v/v) mixture of trifluorethanol and water, as seen by the characteristic minima at 208 nm and 222 nm and a maximum at 190 nm. Assuming an ellipticity of $-40\,000$ deg·cm^2·dmol^{-1} at 220 nm to indicate 100% α helix, the measured value of -19700 and -25700 deg·cm^2·dmol^{-1} at 220 nm for Vpr(13–33) peptide suggests the α helical content averaged over time and sequence to be about 49% and 64% in 100 mM dodecyl-*P*Cho and 50% trifluorethanol, respectively.

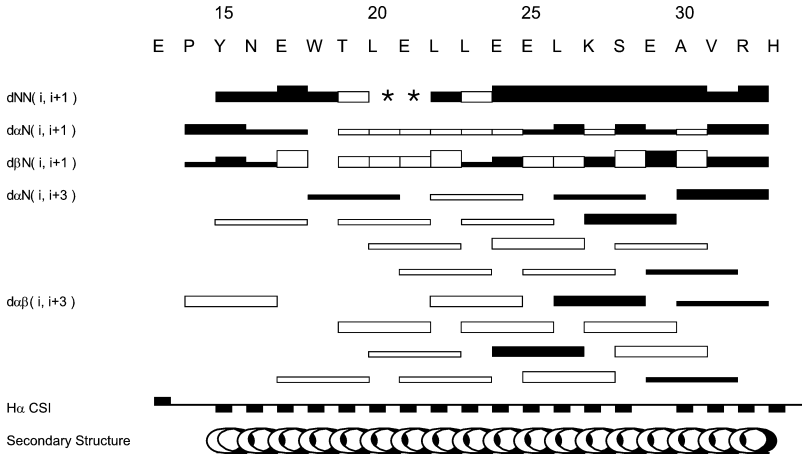

Fig. 4. Summary of the NOE connectivities and chemical shift index analysis of Vpr(13–33). Amino acids are labeled according to the one-letter convention. NOESY connectivities relevant for secondary structure are represented by horizontal rectangles connecting two residues that are related by the NOE specified to the left. The height of the rectangles symbolizes the relative strength (weak, medium, strong) of the cross peaks in a qualitative way. Overlapping and therefore ambiguous cross-peaks not used for structure calculations are marked by open rectangles. Asterisks mark sequential amide crosspeaks expected to appear on the diagonal, and thus are not observable. Hα chemical shift index (CSI) is given below [43].

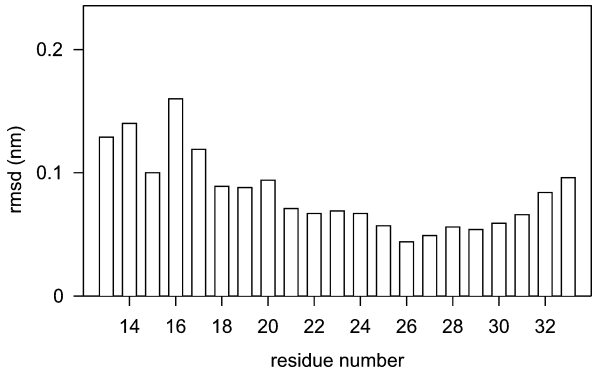

Fig. 5. Root mean square deviation (rmsd) values of the 22 obtained solution structures. For every residue, the rmsd value of the C_α atom was calculated and plotted against the sequence position.

Because trifluorethanol is known to induce helical structure in peptides [22], structural studies in trifluorethanol containing solution may not necessarily yield meaningful results with respect to biological function. Dodecyl-*P*Cho, however, is a suitable membrane mimetic [42]. Thus, our further studies of Vpr(13–33) peptide were carried out in aqueous solution and in the presence of dodecyl-*P*Cho micelles. The amide proton region of the 1D proton NMR spectrum of the peptide in water excludes the presence of peptide monomers with defined structure; recording of 2D spectra did not yield interpretable results, probably due to the presence of high molecular mass aggregates. Successive addition of dodecyl-*P*Cho to the aqueous peptide solution yielded dramatic changes in the NMR spectra and ultimately led to the appearance of well dispersed amide resonances (Fig. 3).

2D NMR spectra (clean-TOCSY, NOESY, DQF-COSY) of a 2.2 mM Vpr(13–33) peptide solution in 100 mM dodecyl-*P*Cho showed satisfactory resolution. By evaluating through-bond connectivities in DQF-COSY and clean-TOCSY spectra, it was possible to identify all spin systems. All resonances could be assigned sequence specifically. Although many of the helix typical NOEs, e.g. $d_{\alpha\beta}(i,i+3)$ and $d_{\alpha N}(i,i+3)$, could not be used for structure calculation due to frequency degeneration (Fig. 4), many other helix indicating NOEs ($i,i+3$ and $i,i+4$) could be identified and used instead (Table 1).

Table 1. Statistics of the structure calculation.

Experimental restraints for the final structure calculation[a]	
Total number of NOEs	190
Intraresidual NOEs $\|i-j\| = 0$	29
Sequential NOEs $\|i-j\| = 1$	80
Medium range NOEs $\|i-j\| = 2,3,4,5$	81
Long range NOEs $\|i-j\| > 5$	0
Molecular dynamics statistics	
Average energy (kca·mol^{-1}) [b]	
E_{tot}	38.56 (± 1.39)
E_{bond}	1.03 (± 0.21)
E_{angle}	29.02 (± 1.07)
E_{impr}	4.66 (± 0.54)
E_{vdw}	1.31 (± 0.98)
E_{NOE}	2.54 (± 0.97)
Rmsd from ideal distances (Å)	
NOE	0.017
Bond length	0.0017
Rmsd from ideal angles (°)	
Bond angles	0.54
Rmsd from 22 structures (Å)	
Backbone	0.85
All non H-Atoms	1.33

[a] The number of each type of constraint is given. None of the 22 structures showed distance violations of more than 0.20 Å. [b] E_{tot}, total energy, E_{repel}, repulsive energy term, E_{NOE}, effective NOE energy term, E_{VDW}, Van der Waals energy term.

A secondary structure estimation employing the chemical shift index strategy (described in [43]) gave further insight into structural features of the peptide. The $C_\alpha H$ chemical shift criteria for helical secondary structure were clearly met for all but the two N-terminal residues (Fig. 4).

It is interesting to note, that for Pro14 and neighbouring residues only one set of resonances could be detected. This indicates that the peptide bond between Pro14 and Glu15

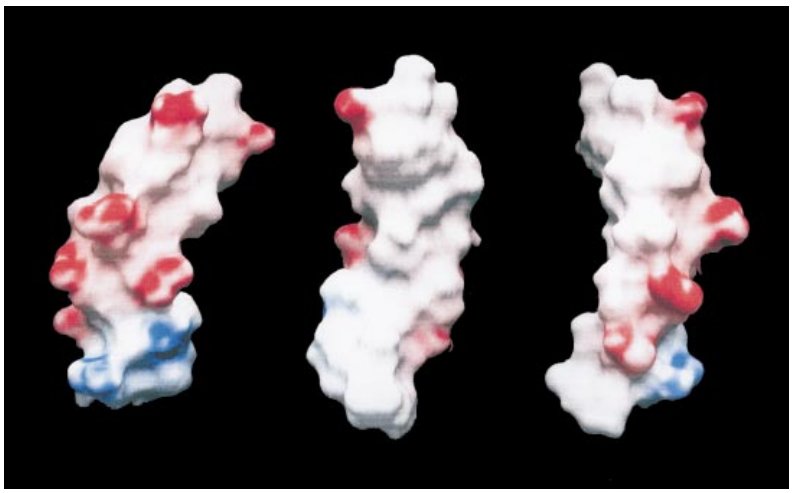

Fig. 6. Representation of Vpr(13–33) structure. The structure of Vpr(13–33) peptide is shown from three different views, rotated about 120 ° against each other. Orientation of the peptide is N-terminus to the top. Positive charges are colored in blue, negative charges are colored in red.

exists exclusively in one conformation, which was determined to be the *trans* conformation.

Simulated annealing and refinement calculations based on agreement with experimental data and ideal geometry yielded 22 structures. The rmsd value of less than 0.1 nm for the entire molecule shows the overall structure to be well defined (Fig. 5). All calculated structures show helical secondary structure for residues 14–33 with an rmsd value of 0.085 nm among the 22 obtained structures. Analysis with the PROCHECK program [37] revealed the presence of regular α helical stretches in all 22 structures, the shortest α helix ranging from amino acids 18–32, and the longest helix observed for amino acids 14–32. PROCHECK analysis yielded for the region of residues 14–17, in most cases regular α helix structure, but also to some extent β turns of types I and IV. This indicates a less defined structure of this part of the molecule. The exclusive *trans* conformation of the peptide bond between Pro14 and Glu15, however, excludes the possibility that this part is completely flexible. In any case, residues 14–17 appear to be helical, but may not form a regular α helix. Taking all the data together, the Vpr(13–33) peptide shows a nicely defined and slightly bent α helix from Pro14 to His33 with strong amphipathic character (Fig. 6).

DISCUSSION

Earlier structural studies of Vpr(1–51) in 30% trifluorethanol containing solution showed a γ turn for residues 14–16, an α helix for residues 17–29, and a β turn type IV for residues 30–33, besides additional structure elements detected in parts outside the region of residues 13–33 [20]. Compared to this study carried out in trifluorethanol-containing solution, we found in Vpr(13–33) a regular α helix from residue 18–32. Residues 14–17 form a helix with imperfect α helical geometry. Both parts build up a slightly bent amphipatic helix comprising residues 14–32.

Our studies in trifluorethanol-free solution show that the 3D structure of Vpr(13–33) in the presence of dodecyl-*P*Cho micelles consists of an amphipathic α helix long enough to span a membrane bilayer. This structural feature is able to easily explain a reported ion chanel activity of Vpr(1–40) [15]. Mutations of either Glu21 or Glu24 to gutamine sigificantly alter selectivity of the ion channel. These residues are located close to each other in the middle of the amphipathic α helix found in the work described here. It is worth mentioning at this point that although all structures obtained from the simulated annealing and refinement calculations showed a slightly bent α helix, it is hard to decide whether this bend is only a consequence of the available constraints. However, recently reported similar studies on the peptaibol chrysospermin C, which is also able to form an ion channel, yielded a slightly bent α helix [44].

Virus particle incorporation of Vpr requires residues 1–47 in the C-terminal p6 region of Gag [45] and residues 17–34 in Vpr [24–26]. Secondary structure prediction of p6 showed a putatative α helical domain within residues 41–46, which resides in the critical portion of p6 important for Vpr packaging. Amphipathic helices are well known to mediate protein–protein interactions [46]. Further, viral packaging takes place near the cytoplasmic membrane. Thus, the amphipathic α helix within Vpr(13–33) might be the critical secondary structure element necessary for virion incorporation of Vpr.

Some residues in Vpr(13–33) are known to be crucial for several Vpr activities. Mutation of Ala30 to leucine completely abolishes G_2 cell cycle arrest and virion packaging of Vpr [23]. Mutations of either Leu23 or Ala30 to phenylalanine dramatically reduce virion incorporation of Vpr but do not interfere with its nuclear localization [24]. One may speculate, that the leucine-zipper like sequence motif preceding Ala30 serves together with helical secondary structure as a basis for a variety of protein–protein interactions between Vpr and other viral and cellular factors. The importance of this secondary structure motif is supported by the finding that mutation of Ala30 to proline abolishes Vpr nuclear localization [23]. Also, mutations of either one of residues Asp17, Glu21, Glu24, Glu25 or Glu29 to proline dramatically reduces virion packaging of Vpr [25].

Vpr does not contain a canonical nuclear localization signal. Nevertheless, Vpr is able to enter the nucleus and to concentrate at nuclear pore complexes. Vpr's function in leading the viral preintegration complex into the nucleus is essential for replication in nondividing cells. To fullfil this function, Vpr needs to be incorporated into virions infecting such cells, because only after entering the nucleus, can viral genes be expressed. Therefore, there are at least two points in the viral life cycle where the structure of Vpr(13–33) can serve as a target for novel antiviral drugs. First, the interaction with p6 for virion packaging, and second, the interaction with components of the nuclear pore complex.

Future structural studies of full-length Vpr in the appropriate environment will give further insights into Vpr function and the molecular mechanisms involved.

ACKNOWLEDGEMENTS

We thank Dr Karl-Heinz Gührs for carrying out mass spectroscopy. This work was supported by a grant from the Deutsche Forschungsgemeinschaft (DFG) to D. W. (SFB 466, A4).

REFERENCES

1. Hoch, J., Lang, S.M., Weeger, M., Stahl Hennig, C., Coulibaly, C., Dittmer, U., Hunsmann, G., Fuchs, D., Muller, J., Sopper, S. *et al.* (1995) vpr deletion mutant of simian immunodeficiency virus induces AIDS in rhesus monkeys. *J. Virol.* **69**, 4807–4813.
2. Lang, S.M., Weeger, M., Stahl Hennig, C., Coulibaly, C., Hunsmann, G., Muller, J., Muller Hermelink, H., Fuchs, D., Wachter, H., Daniel, M.M. *et al.* (1993) Importance of vpr for infection of rhesus monkeys with simian immunodeficiency virus. *J. Virol.* **67**, 902–912.
3. Cohen, E.A., Dehni, G., Sodroski, J.G. & Haseltine, W.A. (1990) Human immunodeficiency virus vpr product is a virion-associated regulatory protein. *J. Virol.* **64**, 3097–3099.
4. Yu, X.F., Matsuda, M., Essex, M. & Lee, T.H. (1990) Open reading frame vpr of simian immunodeficiency virus encodes a virion-associated protein. *J. Virol.* **64**, 5688–5693.
5. Lu, Y.L., Spearman, P. & Ratner, L. (1993) Human immunodeficiency virus type 1 viral protein R localization in infected cells and virions. *J. Virol.* **67**, 6542–6550.
6. Emerman, M. (1996) HIV-1, Vpr and the cell cycle. *Curr. Biol.* **6**, 1096–1103.
7. Heinzinger, N.K., Bukinsky, M.I., Haggerty, S.A., Ragland, A.M., Kewalramani, V., Lee, M.A., Gendelman, H.E., Ratner, L.,

Stevenson, M. & Emerman, M. (1994) The Vpr protein of human immunodeficiency virus type 1 influences nuclear localization of viral nucleic acids in nondividing host cells. *Proc. Natl Acad. Sci. USA* **91**, 7311–7315.

8. Popov, S., Rexach, M., Zybarth, G., Reiling, N., Lee, M.A., Ratner, L., Lane, C.M., Moore, M.S., Blobel, G. & Bukrinsky, M. (1998) Viral protein R regulates nuclear import of the HIV-1 pre-integration complex. *EMBO J.* **17**, 909–917.
9. Levy, D.N., Fernandes, L.S., Williams, W.V. & Weiner, D.B. (1993) Induction of cell differentiation by human immunodeficiency virus 1 vpr. *Cell* **72**, 541–550.
10. He, J., Choe, S., Walker, R., Di Marzio, P., Morgan, D.O. & Landau, N.R. (1995) Human immunodeficiency virus type 1 viral protein R (Vpr) arrests cells in the G2 phase of the cell cycle by inhibiting p34cdc2 activity. *J. Virol.* **69**, 6705–6711.
11. Jowett, J.B., Planelles, V., Poon, B., Shah, N.P., Chen, M.L. & Chen, I.S. (1995) The human immunodeficiency virus type 1 vpr gene arrests infected T cells in the G2 + M phase of the cell cycle. *J. Virol.* **69**, 6304–6313.
12. Re, F., Braaten, D., Franke, E.K. & Luban, J. (1995) Human immunodeficiency virus type 1 Vpr arrests the cell cycle in G2 by inhibiting the activation of p34cdc2-cyclin B. *J. Virol.* **69**, 6859–6864.
13. Rogel, M.E., Wu, L.I. & Emerman, M. (1995) The human immunodeficiency virus type 1 vpr gene prevents cell proliferation during chronic infection. *J. Virol.* **69**, 882–888.
14. Piller, S.C., Ewart, G.D., Premkumar, A., Cox, G.B. & Gage, P.W. (1996) Vpr protein of human immunodeficiency virus type 1 forms cation-selective channels in planar lipid bilayers. *Proc. Natl Acad. Sci. USA.* **93**, 111–115.
15. Piller, S.C., Ewart, G.D., Jans, D.A., Gage, P.W. & Cox, G.B. (1999) The amino-terminal region of Vpr from human immunodeficiency virus type 1 forms ion channels and kills neurons. *J. Virol.* **73**, 4230–4238.
16. Bouhamdan, M., Benichou, S., Rey, F., Navarro, J.M., Agostini, I., Spire, B., Camonis, J., Slupphaug, G., Vigne, R., Benarous, R. & Sire, J. (1996) Human immunodeficiency virus type 1 Vpr protein binds to the uracil DNA glycosylase DNA repair enzyme. *J. Virol.* **70**, 697–704.
17. Withers-Ward, E.S., Jowett, J.B., Stewart, S.A., Xie, Y.M., Garfinkel, A., Shibagaki, Y., Chow, S.A., Shah, N., Hanaoka, F., Sawitz, D.G., Armstrong, R.W., Souza, L.M. & Chen, I.S. (1997) Human immunodeficiency virus type 1 Vpr interacts with HHR23A, a cellular protein implicated in nucleotide excision DNA repair. *J. Virol.* **71**, 9732–9742.
18. Refaeli, Y., Levy, D.N. & Weiner, D.B. (1995) The glucocorticoid receptor type II complex is a target of the HIV-1 vpr gene product. *Proc. Natl Acad. Sci. USA* **92**, 3621–3625.
19. Vodicka, M.A., Koepp, D.M., Silver, P.A. & Emerman, M. (1998) HIV-1 Vpr interacts with the nuclear transport pathway to promote macrophage infection. *Genes Dev.* **12**, 175–185.
20. Wecker, K. & Roques, B.P. (1999) NMR structure of the (1–51) N-terminal domain of the HIV-1 regulatory protein Vpr. *Eur. J. Biochem.* **266**, 359–369.
21. Schüler, W., Wecker, K., de Rocquigny, H., Baudat, Y., Sire, J. & Roques, B.P. (1999) NMR structure of the (52–96) C-terminal domain of the HIV-1 regulatory protein Vpr: molecular insights into its biological functions. *J. Mol. Biol.* **285**, 2105–2117.
22. Sönnichsen, F.D., Van Eyk, J.E., Hodges, R.S. & Sykes, B.D. (1992) Effect of trifluoroethanol on protein secondary structure: an NMR and CD study using a synthetic actin peptide. *Biochemistry.* **31**, 8790–8798.
23. Di Marzio, P., Choe, S., Ebright, M., Knoblauch, R. & Landau, N.R. (1995) Mutational analysis of cell cycle arrest, nuclear localization and virion packaging of human immunodeficiency virus type 1 Vpr. *J. Virol.* **69**, 7909–7916.
24. Yao, X.J., Subbramanian, R.A., Rougeau, N., Boisvert, F., Bergeron, D. & Cohen, E.A. (1995) Mutagenic analysis of human immunodeficiency virus type 1 Vpr: role of a predicted N-terminal alpha-helical structure in Vpr nuclear localization and virion incorporation. *J. Virol.* **69**, 7032–7044.
25. Mahalingam, S., Khan, S.A., Murali, R., Jabbar, M.A., Monken, C.E., Collman, R.G. & Srinivasan, A. (1995) Mutagenesis of the putative alpha-helical domain of the Vpr protein of human immunodeficiency virus type 1: effect on stability and virion incorporation. *Proc. Natl Acad. Sci. USA* **92**, 3794–3798.
26. Mahalingam, S., Khan, S.A., Jabbar, M.A., Monken, C.E., Collman, R.G. & Srinivasan, A. (1995) Identification of residues in the N-terminal acidic domain of HIV-1 Vpr essential for virion incorporation. *Virology.* **207**, 297–302.
27. Chen, M., Elder, R.T., Yu, M., O'Gorman, M.G., Selig, L., Benarous, R., Yamamoto, A. & Zhao, Y. (1999) Mutational analysis of Vpr-induced G2 arrest, nuclear localization, and cell death in fission yeast. *J. Virol.* **73**, 3236–3245.
28. Rance, M., Sørensen, O.W., Bodenhausen, G., Wagner, G., Ernst, R.R. & Wüthrich, K. (1983) Improved spectral resolution in COSY ^{1}H NMR spectra of proteins via double quantum filtering. *Biochem. Biophys. Res. Commun.* **117**, 479–485.
29. Braunschweiler, L. & Ernst, R.R. (1983) Coherence transfer by istropic mixing: Application to proton correlation spectroscopy. *J. Magn. Reson.* **53**, 521–528.
30. Shaka, A.J., Lee, C.J. & Pines, A. (1988) Iterative schemes for bilinear operators; application to spindecoupling. *J. Magn. Reson.* **77**, 274–293.
31. Kraulis, J., Clore, G.M., Nilges, M., Jones, T.A., Pettersson, G., Knowles, J. & Gronenborn, A.M. (1989) Determination of the three-dimensional solution structure of the C-terminal domain of cellobiohydrolase I from *Trichoderma reesei*. A study using nuclear magnetic resonance and hybrid distance geometry-dynamical simulated annealing. *Biochemistry.* **28**, 7241–7257.
32. Brünger, A.T. (1993) *XPLOR, Version 3.1.* Howard Hughes Medical Institute & Yale University, New Haven, CT, USA.
33. Kharrat, A., Macias, M.J., Gibson, T.J., Nilges, M. & Pastore, A. (1995) Structure of the dsRNA binding domain of *E. coli* RNase III. *EMBO J.* **14**, 3572–3584.
34. Kemmink, J., Darby, N.J., Dijkstra, K., Nilges, M. & Creighton, T.E. (1996) Structure determination of the N-terminal thioredoxin-like domain of protein disulfide isomerase using multidimensional heteronuclear ^{13}C/^{15}N NMR spectroscopy. *Biochemistry.* **35**, 7684–7691.
35. Holak, T.A., Nilges, M. & Oschkinat, H. (1989) Improved strategies for the determination of protein structures from NMR data: the solution structure of acyl carrier protein. *FEBS Lett.* **242**, 218–224.
36. Nilges, M. (1993) A calculation strategy for the structure determination of symmetric dimers by ^{1}H NMR. *Proteins.* **17**, 297–309.
37. Laskowski, R.A., MacArthur, M.W. & Thornton, J.M. (1993) PROCHECK: a program to check the stereochemical quality of protein structures. *J. Appl. Crystallog.* **26**, 283–291.
38. Hutchinson, E.G. & Thornton, J.M. (1996) PROMOTIF – a program to identify and analyze structural motifs in proteins. *Protein Sci.* **5**, 212–220.
39. Nie, Z., Bergeron, D., Subbramanian, R.A., Yao, X.J., Checroune, F., Rougeau, N. & Cohen, E.A. (1998) The putative alpha helix 2 of human immunodeficiency virus type 1 Vpr contains a determinant which is responsible for the nuclear translocation of proviral DNA in growth-arrested cells. *J. Virol.* **72**, 4104–4115.
40. Subbramanian, R.A., Yao, X.J., Dilhuydy, H., Rougeau, N., Bergeron, D., Robitaille, Y. & Cohen, E.A. (1998) Human immunodeficiency virus type 1 Vpr localization: nuclear transport of a viral protein modulated by a putative amphipathic helical

structure and its relevance to biological activity. *J. Mol. Biol.* **278**, 13–30.
41. Rost, B., Sander, C., Pope, B. & Kent, H.M. (1993) Prediction of protein secondary structure at better than 70% accuracy. *J. Mol. Biol.* **232**, 584–599.
42. Vinogradova, O., Sonnichsen, F. & Sanders, C.R. 2nd. (1998) On choosing a detergent for solution NMR studies of membrane proteins. *J. Biomol. NMR.* **11**, 381–386.
43. Wishart, D.S., Sykes, B.D. & Richards, F.M. (1992) The chemical shift index: a fast and simple method for the assignment of protein secondary structure through NMR spectroscopy. *Biochemistry* **31**, 1647–1651.
44. Anders, R., Ohlenschlager, O., Soskic, V., Wenschuh, H., Heise, B. & Brown, L.R. (2000) The NMR solution structure of the ion channel peptaibol chrysospermin C bound to dodecylphosphocholine micelles. *Eur. J. Biochem.* **267**, 1784–1794.
45. Kondo, E., Mammano, F., Cohen, E.A. & Gottlinger, H.G. (1995) The p6gag domain of human immunodeficiency virus type 1 is sufficient for the incorporation of Vpr into heterologous viral particles. *J. Virol*. **69**, 2759–2764.
46. Segrest, J.P., Loof, H., Dohlman, J.G., Brouillette, C.G. & Anantharamaiah, G.M. (1990) Amphipathic helix motif: classes and properties. *Proteins* **8**, 103–117.

SUPPLEMENTARY MATERIAL

The following material is available from
http://www.blackwell-science.com/ejb
Table S1. NMR chemical shifts of Vpr(13–33) peptide in aqueous 100 mM dodecylphosphocholine at 298 K calibrated to 2,2-dimethyl-2-silapentanesulfonate.